Two-dimensional solitons and vortices in normal and anomalous dispersive media

T. A. Davydova,* A. I. Yakimenko,† and Yu. A. Zaliznyak‡
Institute for Nuclear Research, Prospect Nauki 47, Kiev 03680, Ukraine
(Received 16 September 2002; published 5 February 2003)

We study solitons and vortices described by the $(2+1)$-dimensional fourth-order generalized nonlinear Schrödinger equation with cubic-quintic nonlinearity. Necessary conditions for the existence of such structures are investigated analytically using conservation laws and asymptotic behavior of localized solutions. We derive the generalized virial relation, which describes the combined influence of linear and nonlinear effects on the evolution of the wave packet envelope. By means of refined variational analysis, we predict the main features of steady soliton solutions, which have been shown to be in good agreement with our numerical results. Soliton and vortex stability is investigated by linear analysis and direct numerical simulations. We show that stable bright solitons exist in nonlinear Kerr media both in anomalous and normal dispersive regimes, even if only the fourth-order dispersive effect is taken into account. Vortices occur robust with respect to symmetry-breaking azimuthal instability only in the presence of additional defocusing quintic nonlinearity in the strongly nonlinear regime. We apply our results to the theoretical explanation of whistler self-induced waveguide propagation in plasmas, and discuss possible applications to light beam propagation in cubic-quintic optical materials and to solitons in two-dimensional molecular systems.

DOI: 10.1103/PhysRevE.67.026402 PACS number(s): 52.35.Mw, 42.65.Tg

I. INTRODUCTION

Various types of solitons and vortex solitons (vortices) have been observed experimentally in different dispersive media: gravity waves in deep water [1], electromagnetic waves in plasmas [2–9], ultrashort light waves in optical waveguides (fibers) [10–12], light beams in self-defocusing [13,14] and self-focusing media [15,16], spin waves in ferromagnetic films [17]. These structures may be of the ''bright'' form, localized in space or time (spatial or temporal solitons), or generally both in space and time. Also they may be of the ''dark'' form, as dark holes embedded on a carrier wave background. Vortex solitons have a phase circulation around the axis of propagation, which is equal to $2\pi m$. Integer m is called a topological charge. Ordinary solitons have zero topological charge. Unlike ordinary solitons, vortices have nonzero angular momentum and phase singularity in a wave front.

Optical solitons are considered now as probable elements for ultrahigh speed and effectively lossless communication systems in the near future [12]. Stable solitons are believed to play an important role for the transport of energy or electrons in different one-dimensional (1D) [18–20] and 2D molecular (in particular, biological) systems [16,21,22]. Despite the diversity of physical systems, where solitons and vortices have been observed, they reveal some universal features. They generally appear above some threshold of wave intensity if linear dispersive (diffraction) effects and nonlinear effects balance each other. One-dimensional and two-dimensional structures frequently exhibit an instability in higher space dimensions. This instability may give rise to nonlinear structures of higher dimension space. One of the most popular and universal models describing the nonlinear evolution of a wave envelope and, in particular, the possibility of stable coherent structure formation is the nonlinear Schrödinger equation (NSE). We will be interested further only in 2D localized structures, based on the so-called $(2+1)$-dimensional NSE equation with some additional terms. As is well known, the ordinary 2D NSE

$$i\frac{\partial\Psi}{\partial t}+D\Delta_{\perp}\Psi+B|\Psi|^2\Psi=0 \tag{1}$$

(where $\Delta_{\perp}$ is a 2D Laplacian operator) describes spatial-temporal dynamics of the wave packet envelope due to a competition of the lowest-order dispersive and nonlinear self-interaction terms. It is also widely applied to a problem of stationary (in time) propagation of bounded electromagnetic beams along some direction z in the so-called paraxial approximation. In this case, the time variable t is replaced by z in the basic dimensionless NSE (1). In the following, we will refer to the variable t as time for definiteness. It is also well known (see, for example, Ref. [16]) that in the case $DB>0$, NSE (1) has only an unstable soliton solution, which either disperses or collapses. And it has no soliton solutions at all if $DB<0$. However, many experimental data, where solitons have been observed, contradict the above theoretical conclusions based on Eq. (1) in both cases [3,8,16]. The first case ($DB>0$) is usually [23] referred to as anomalous dispersive media (positive group velocity dispersion, $\partial v_g/\partial k>0$) and the second one ($DB<0$) is referred to as normal dispersive media (negative group velocity dispersion, $\partial v_g/\partial k<0$).

The problem of steady-state self-focusing in nonlinear optics [16,24] and plasma physics [25,26] in anomalous dispersive regime ($DB>0$) was usually considered taking into account some kind of saturable nonlinearity. A refractive index $n(|\Psi|^2)$ can be approximated by

*Electronic address: tdavyd@kinr.kiev.ua
†Electronic address: ayakim@kinr.kiev.ua
‡Electronic address: zalik@kinr.kiev.ua

$$n(|\Psi|^2)=n_0+n_2|\Psi|^2+n_4|\Psi|^4, \quad (2)$$

where constants n_2 and n_4 ($n_2n_4<0$) determine the nonlinear response of the media with small wave beam intensity $|\Psi|^2$. The dependence (2) may be good enough for some optical materials [27] even for intensities above the critical value $|\Psi_{cr}|^2=|n_2/(2n_4)|$ when the derivative $\partial n/\partial|\Psi|^2$ changes its sign. For a problem of wave beam propagation, this corresponds to a change of the self-focusing regime by the self-defocusing one. A variety of bright soliton and vortex solutions has been found using cubic-quintic NSE with anomalous dispersion, and much attention has been paid to the question of their stability [16]. Spatial solitons have been observed since 1965 in many optical media [16]. They correspond to a stationary wave propagation in a self-induced waveguide with the intensity profile unchanged along the direction of wave propagation. The 2D vortex was experimentally created by passing the laser beam through a diffracting planar phase mask [15]. The other important nonlinear stabilizing effect to NSE solitons is given by defocusing nonlocal nonlinearities, which are essential for different electromagnetic waves in plasmas [28–30], for solitons in molecular systems [18,20,21] and in many other applications [31].

On the other hand, as was stressed by Karpman [32,33], effects of higher-order dispersion may also play a significant role. The additional fourth-order dispersion term to NSE (1) may be essential for electrostatic waves [29,30] and electromagnetic waves, when two wave polarizations are taken into account, in magnetized plasma [34]. It may be produced by a nonlocal nonlinear dispersion [20] and in higher-order quasicontinuum models, which approximate discreteness in condensed matter physics [16]. It was shown in Refs. [32,33] that in the anomalous dispersive regime ($DB>0$) the fourth-order dispersive term of the form $P\Delta^2\Psi$ leads to an existence of stable localized soliton solution if $PD<0$. The presence of two light polarizations has been considered in Ref. [35] for nonlinear optical media using vectorlike cubic-quintic NSE, where stable solitons ($m=0$) and vortices ($m=1$ and $m=2$) have been discovered. Many other effects may also lead to a collapse arresting and to an appearance of stable 2D solitons and vortices, which have been discussed in literature. However, higher-order linear and nonlinear effects have mostly been studied separately for the 2D NSE.

To our knowledge, there is no theory to explain that experimental data have indicated stationary self-induced waveguide propagation of electromagnetic waves [3,8] in the case of normal dispersion ($DB<0$). In the presence of additional quintic nonlinearity, described by a term of the form $K|\Psi|^4\Psi$ with $DK<0$, soliton solutions of Eq. (1) are unstable even in the 1D case. The conditions for the existence of stable soliton solutions have been revealed for 1D NSE with $BD<0$ in the presence of quintic nonlinearity plus the fourth-order dispersion [36]. Though 1D and 2D systems are rather different, one can expect that stable localized structures may exist also in the 2D case with $BD<0$, when higher-order dispersion is taken into account. We will show that the fourth-order dispersion can prevent a collapse and really gives rise to the stable 2D soliton (waveguide) formation and even to stable vortices in the presence of cubic-quintic nonlinearity.

The key question is what corrections to NSE are most essential. In a typical physical situation, when a wave beam self-contracts, its field intensity increases (due to energy conservation, if strong dissipative processes are absent). For the 2D NSE with $BD>0$, both additional nonlinear and linear effects can separately determine the stability of 2D solitons [24,37], though they act together and could be of equal importance. For the 2D NSE with $BD<0$, we will determine the appropriate model describing solitons and vortices in this paper.

Here, we consider conditions for the formation of coherent structures and their stability on the basis of the generalized NSE (GNSE) including second- and fourth-order dispersion effects and cubic-quintic nonlinearity:

$$i\frac{\partial\Psi}{\partial t}+D\Delta_\perp\Psi+P\Delta_\perp^2\Psi+B|\Psi|^2\Psi+K|\Psi|^4\Psi=0. \quad (3)$$

We will study GNSE (3) both in anomalous ($DB>0$) and in normal ($DB<0$) dispersive regimes. We are mostly interested in the case where $BK<0$ (which corresponds to saturable cubic-quintic nonlinearity) and $PK>0$ (when collapse can be prevented). The main purpose of this paper is to investigate the influence of a combination of higher-order dispersion and saturation of nonlinearity on the features of localized solitons and vortices as well as to reveal the role of each of these supplementary effects.

Our paper is organized as follows. In Sec. II we describe our model, analyze some general dynamical properties of localized solutions, and reveal necessary conditions for soliton existence. We obtain the virial relation for GNSE (3), which generalizes the well known relation [38] to the case $P\neq0$, and show that in the case $PK>0$, wave collapse is not expected. We investigate properties of solitons and m-charged vortices ($m=1,2$) in Secs. III and IV for different dispersive regimes. For this purpose, we have used a variational approach, taking into account the changing of soliton spatial form with its energy (number of quanta). Numerical calculations have shown very good agreement with our variational approach. We have also analyzed analytically and numerically the stability of solitons and vortices with respect to radial and azimuthal perturbations. The role of higher-order dispersion and quintic nonlinearity on the stability of solitons and vortices, and their properties have been found to be quite different in anomalous and in normal dispersion regimes. In Sec. V, we make conclusions and discuss some applications of our results to plasma physics, nonlinear optics, and molecular systems.

II. GENERAL PROPERTIES OF LOCALIZED STRUCTURES IN THE FRAMEWORK OF GNSE

We consider here wave packet evolution and stationary localized structures in the framework of GNSE (3), which takes into account the second- and fourth-order dispersion effects (terms proportional to D and P, respectively). Two

last terms, proportional to B and K, describe cubic and quintic nonlinearities. Our concern is only with the localized solutions $\Psi(x,y,t)$, for which the following integrals of motion are finite:

(i) Number of quanta (''energy'' or ''beam power'')

$$N=\int |\Psi|^2 d^2\mathbf{r}. \tag{4}$$

(ii) x and y components of momentum:

$$\vec{I}=-\frac{i}{2}\int (\Psi^*\nabla\Psi-\Psi\nabla\Psi^*)d^2\mathbf{r}, \tag{5}$$

(iii) z component of angular momentum:

$$\vec{M}=-\frac{i}{2}\int (\Psi^*[\mathbf{r}\times\nabla\Psi]-\Psi[\mathbf{r}\times\nabla\Psi^*])d^2\mathbf{r}, \tag{6}$$

(iv) Hamiltonian

$$\begin{aligned} H&=D\int |\nabla\Psi|^2 d^2\mathbf{r}-P\int |\Delta_\perp\Psi|^2 d^2\mathbf{r}\\ &\quad-\frac{1}{2}B\int |\Psi|^4 d^2\mathbf{r}-\frac{1}{3}K\int |\Psi|^6 d^2\mathbf{r}\\ &\equiv DI_D-PI_P-\tfrac{1}{2}BI_B-\tfrac{1}{3}KI_K. \end{aligned} \tag{7}$$

We will consider localized stationary solutions in two different cases.

(a) The so-called anomalous dispersive regime:

$$DB>0, \quad PK>0, \quad PB<0, \quad D<0. \tag{8}$$

(b) The normal dispersive regime:

$$DB<0, \quad PK>0, \quad PB<0, \quad D>0. \tag{9}$$

To make it definite, we put $D<0$ in case (a) and $D>0$ in case (b), meaning some physical applications (see the Appendix). To avoid misunderstanding, we will refer to the anomalous or normal dispersive regime by indicating the sign of the product DB in line with the usually accepted rule [23].

In accordance with Lyapunov's theorem, for the bounded functional H of field variables Ψ (sufficiently for other integrals of motion fixed: N, $\vec{I}_\perp$, M_z) there exists a stable soliton solution that realizes its maximum or minimum (see, e.g., Refs. [37,39]).

Using the inequalities

$$I_D\leqslant (NI_P)^{1/2} \tag{10}$$

and

$$I_B\leqslant (NI_K)^{1/2}, \tag{11}$$

for integrals defined in Eq. (7), it is easy to show that the functional H is bounded from above, at fixed N, in both cases under consideration. Indeed, one can find the following estimate for the Hamiltonian (7) in the normal dispersive regime (9):

$$\begin{aligned} H&\leqslant D(NI_P)^{1/2}-PI_P+\frac{1}{2}|B|(NI_K)^{1/2}-\frac{1}{3}KI_K\\ &\leqslant \frac{N}{4}\left[\frac{D^2}{P}+\frac{3}{4}\frac{B^2}{K}\right]. \end{aligned} \tag{12}$$

For the anomalous dispersive regime (8) one obtains the more strict estimate

$$H\leqslant \frac{3NB^2}{16K}. \tag{13}$$

In Sec. II B we will show that the Hamiltonian is positive for any localized stationary solution of GNSE (3) in cases (8) and (9). Thus, in both dispersive regimes there exists at least one stable soliton solution.

A. Virial relation

Some insight about a combined action of linear and nonlinear effects on the evolution of a wave packet envelope and necessary conditions for an existence of localized stationary solutions can be obtained using virial relation for the effective square beam width $r_{\rm eff}^2$. The latter is defined by the relation

$$r_{\rm eff}^2=\frac{1}{N}\int r^2|\Psi|^2 d^2\mathbf{r}, \tag{14}$$

where $r=\sqrt{x^2+y^2}$. We have generalized the known virial relation [see, e.g., Ref. [38] for GNSE (3) with $P=0$] to the more general Eq. (3) with $P\neq 0$. This virial relation may be written as

$$\begin{aligned} \frac{N}{8}\frac{d^2r_{\rm eff}^2}{dt^2}&=\int\left\{D^2|\nabla\Psi|^2-4DP|\Delta_\perp\Psi|^2+4P^2|\nabla\Delta_\perp\Psi|^2\right.\\ &\quad-D|\Psi|^4\left(\frac{B}{2}+\frac{2K}{3}|\Psi|^2\right)-rP\left[\left(|\nabla\Psi|^2\right.\right.\\ &\quad\left.\left.+2\left|\frac{\partial\Psi}{\partial r}\right|^2\right)\frac{\partial}{\partial r}(B|\Psi|^2+K|\Psi|^4)\right.\\ &\quad\left.\left.+2K(\nabla|\Psi|)^2\frac{\partial|\Psi|^4}{\partial r}\right]\right\}d^2\mathbf{r}\\ &=f_{\rm eff}. \end{aligned} \tag{15}$$

From Eq. (15) one finds that (i) when $P=K=0$ and $BD<0$, GNSE (3) has no localized solutions at all, any wave packet spreads out in the radial direction; (ii) in the case $P=0$, $K\neq 0$ virial relation (15) gives both in the cases $BD>0$ and $BD<0$ that

$$N\frac{d^2r_{\rm eff}^2}{dt^2}=8D\left(H-\frac{1}{3}KI_K\right),$$

and predicts the collapse of any wave packet having $DH<0$, $DK>0$; (iii) the sum of all linear terms, proportional to D^2, $DP>0$, and P^2 in the virial relation, is defocusing because

$$f_{\text{eff}} \geqslant \frac{[DI_D - PI_P]^2}{I_D} > 0. \tag{16}$$

This estimate follows from the integral inequality

$$I_P < \left(I_D \int |\nabla \Delta_\perp \Psi|^2 d^2\mathbf{r} \right)^{1/2}. \tag{17}$$

If $DP<0$, it is trivial that $f_{\text{eff}}>0$. Thus, any wave packet in the linear approximation ($B=K=0$) has a trend to asymptotically (at $t\to\infty$) spread out. In the limiting case $P=0$ and $D\neq 0$, it was found in Ref. [23] that

$$\frac{d^2 r_{\text{eff}}^4}{dt^2} \geqslant r_{\text{eff}}^2 \frac{d^2 r_{\text{eff}}^2}{dt^2} \geqslant 16D^2,$$

where the virial relation (15) and the ''uncertainty principle''

$$r_{\text{eff}}^2 I_D \geqslant N \tag{18}$$

were used. Hence

$$r_{\text{eff}}^4(t) \geqslant 8D^2 t^2 + 2t r_{\text{eff}}^2(0) \left. \frac{dr_{\text{eff}}^2}{dt} \right|_{t=0} + r_{\text{eff}}^2(0).$$

Thus, r_{eff}^2 asymptotically diverges at $t\to\infty$, at least as $\sqrt{8}|D|t$, if $r_{\text{eff}}(0)|(dr_{\text{eff}}^2/dt)_{t=0}| < \sqrt{8}|D|$.

From inequalities

$$\frac{1}{4}\frac{d^2}{dt^2}(r_{\text{eff}}^2)^4 > (r_{\text{eff}}^2)^3 \frac{d^2 r_{\text{eff}}^2}{dt^2} > 32P^2, \tag{19}$$

we have similarly found that a wave packet described by the GNSE with $P\neq 0$, $D=B=K=0$ will asymptotically spread out not slower than according to the law $r_{\text{eff}}^2 \sim 2\sqrt[4]{8}\sqrt{|P|}t$. To obtain Eq. (19) we have used the relation

$$\int |\nabla \Delta_\perp \Psi|^2 d^2\mathbf{r} \geqslant I_P^2 / I_D \geqslant N/(r_{\text{eff}}^2)^3,$$

which is derived by taking into account inequalities (10), (17), and (18).

If $BP<0$, $PK>0$ the virial relation includes focusing (proportional to BP) as well as defocusing (proportional to PK) nonlinear terms. Thus, it is natural to expect that stationary nonlinear structures can exist in the framework of GNSE (3), both in anomalous [Eq. (8)] and in normal [Eq. (9)] dispersive regimes.

From scaling arguments one can expect that any wave packet is unable to collapse if $PK>0$. Actually, two terms, namely, those proportional to P^2 and to PK in expression (15), would grow faster, than any other terms could change, if a wave packet contracted. Such a repulsive ''force'' $f_{\text{eff}}>0$ makes self-similar global collapse impossible.

As known [37], in the presence of the fourth-order dispersion ($P\neq 0$), the ''centroid''

$$\langle \mathbf{r} \rangle = \frac{1}{N} \int \mathbf{r} |\Psi|^2 d^2\mathbf{r} \tag{20}$$

generally moves nonuniformly because GNSE (3) is not Galilean invariant. We will consider only the case when the centroid, located at $r=0$, is immobile, so that the radial component of momentum (5) is equal to zero. This is a typical situation for a problem of wave beam propagation.

B. Stationary solutions of GNSE

We consider now stationary localized structures, which may appear as the result of a balance of wave packet dispersion spreading and nonlinear compression. We are looking for a steady-state solution of the form

$$\Psi(\mathbf{r},t) = \hat{\Psi}(\mathbf{r}) e^{i\Lambda t}, \tag{21}$$

where Λ is the nonlinear frequency shift. The function $\hat{\Psi}(\mathbf{r})$ obeys the partial differential equation

$$-\Lambda\hat{\Psi} + D\Delta_\perp \hat{\Psi} + P\Delta_\perp^2 \hat{\Psi} + B|\hat{\Psi}|^2\hat{\Psi} + K|\hat{\Psi}|^4\hat{\Psi} = 0. \tag{22}$$

As known, Eq. (22) may be obtained from the constrained variational problem for the Hamiltonian: $\delta(H+\Lambda N)=0$. Thus, the steady-state solution of the form (21) is a stationary point of the Hamiltonian H at a fixed number of quanta.

One yields a useful integral relation for steady-state solutions, multiplying Eq. (22) by $\hat{\Psi}^*$ and integrating over space coordinates:

$$\Lambda N = PI_P - DI_D + BI_B + KI_K, \tag{23}$$

where the integrals I_D, I_P, I_B, and I_K are defined in Eq. (7). Multiplying Eq. (22) by $r^2 \partial\hat{\Psi}^*/\partial r$, integrating and adding the complex conjugate, another integral identity is found:

$$\Lambda N = -PI_P + BI_B/2 + KI_K/3. \tag{24}$$

Excluding Λ from Eqs. (23) and (24) one finds the following expressions for the Hamiltonian, valid for stationary solutions:

$$H = PI_P + KI_K/3 = DI_D/2 - BI_B/4. \tag{25}$$

One can see that the Hamiltonian is positive for any stationary solution of Eq. (22) in two regimes (8) and (9), because $P>0$ and $K>0$. Taking into account estimates (12) and (13) for Hamiltonian (7), one concludes that in both regimes there exists a stable stationary localized solution, which corresponds to the Hamiltonian's global extremum.

Using Eqs. (23) and (24) and excluding terms proportional to K, it is straightforward to find that the nonlinear frequency shift Λ is negative for a stationary solution in the anomalous dispersive regime (8). Furthermore, in the normal

dispersive regime (9) with $DP>0$, the wave packet would lose its energy, due to a resonant radiation of linear waves [37,40] with dispersion $\omega(k)=Dk^2-Pk^4$, if the nonlinear frequency shift could be such that $\Lambda>-D^2/4P$. Thus, the radiationless stationary wave packet should have $\Lambda<-D^2/(4P)$ in regime (9). Note that, owing to the negative value of Λ, stationary solutions are radiationless in the anomalous dispersive regime (8) too.

To estimate how the nonlinear frequency shift Λ is restricted from below, we have used inequalities (10) and (11). Excluding terms proportional to P from integral equalities (23), (24), we obtain $\Lambda>-\frac{27}{128}B^2/K$ in the regime (8). And in the regime (9) we obtain from Eq. (23) that $\Lambda>-D^2/4P-B^2/4K$.

Hence, the nonlinear frequency shift Λ of a steady-state radiationless localized solution (21) is bounded from below and above for both dispersion regimes. One obtains in the anomalous dispersive regime,

$$-\frac{27}{128}\frac{B^2}{K}<\Lambda<0, \tag{26}$$

and in the normal dispersive regime,

$$-\frac{D^2}{4P}-\frac{B^2}{4K}<\Lambda<-\frac{D^2}{4P}. \tag{27}$$

Further, we are looking for stationary solutions of the following form:

$$\Psi(\mathbf{r},t)=\psi(r)e^{\mathrm{i}m\varphi+\mathrm{i}\Lambda t}, \tag{28}$$

where φ is the azimuthal angle, integer m is the topological charge. Solutions of the form (28), with $m=0$ are called *solitonlike* (or solitons) and solutions with $m\neq 0$ are called *vortexlike* (or vortices). A simple "quantization rule" $M_z=mN$ is fulfilled for the angular momentum of such solutions.

The radial function $\psi(r)$ satisfies the ordinary differential equation

$$-\Lambda\psi+D\Delta_r^{(m)}\psi+P(\Delta_r^{(m)})^2\psi+B|\psi|^2\psi+K|\psi|^4\psi=0, \tag{29}$$

where the operator $\Delta_r^{(m)}$ is given by

$$\Delta_r^{(m)}=\frac{d^2}{dr^2}+\frac{1}{r}\frac{d}{dr}-\frac{m^2}{r^2}.$$

The stationary equation (29) should be complemented by boundary conditions at $r=0$ and at infinity. A solitonlike solution is an even function of r, therefore the first pair of boundary conditions for a solution with $m=0$ is

$$\left.\frac{d\psi(r)}{dr}\right|_{r=0}=0, \quad \left.\frac{d}{dr}\Delta_r^{(0)}\psi(r)\right|_{r=0}=0. \tag{30}$$

A vortexlike solution has the following asymptotic behavior at $r\to 0$: $\psi(r)\sim h_m r^{|m|}$, where $h_m=\mathrm{const}$. Thus, the vortices ($m\neq 0$) satisfy the conditions

$$\psi(0)=0, \quad \Delta_r^{(m)}\psi(r)|_{r=0}=0. \tag{31}$$

The second pair of boundary conditions for localized solutions is

$$\lim_{r\to\infty}\psi(r)=0, \quad \lim_{r\to\infty}[\Delta_r^{(m)}\psi(r)]=0. \tag{32}$$

We will now consider the asymptotic behavior of localized solutions at infinity more carefully. The solutions of linearized (at $r\to\infty$) Eq. (29) have asymptotes of the form $h_i r^{-1/2}e^{\mathrm{i}k_i r}$, where k_i are solutions of the following equation:

$$-\Lambda-k^2D+k^4P=0 \tag{33}$$

and are given by

$$k=\pm\sqrt{\frac{D}{2P}\{1\pm\sqrt{1+4\Lambda P/D^2}\}}. \tag{34}$$

A localized solution should have $\mathrm{Im}k>0$. If $DP<0$ [regime (8)] this condition is fulfilled for any $\Lambda<0$. If $DP>0$ [regime (9)] the condition $\mathrm{Im}k>0$ leads to a further restriction on nonlinear frequency shift: $\Lambda<-D^2/4P$. Thus, we have found that in both regimes under consideration, the condition of absence of radiation is fulfilled automatically for any localized solution. It is seen from Eq. (34) that $\mathrm{Re}k\neq 0$ for $\Lambda<-D^2/4P$, and so in this case the radial function $\psi(r)$ has "oscillating tails." These tails are especially noticeable for the solution of GNSE (29) at $DP>0$ when $\Lambda\approx-D^2/4P$. In this case $\mathrm{Im}k$ occurs small compared to $\mathrm{Re}k$, hence the function $\psi(r)$ slowly decreases at infinity ($\mathrm{Im}k\to 0$ if $\Lambda\to-D^2/4P$), while its spatial frequency of oscillations remains finite ($\mathrm{Re}k\to\sqrt{D/2P}$).

In the special case $P=0$, we see from Eq. (33) that $k^2=-\Lambda/D$ and $\mathrm{Im}k\neq 0$ only if $\Lambda D>0$. But, for any stationary radiationless solution, the nonlinear frequency shift Λ is negative. Thus, there is no robust localized solution in the normal dispersive regime (9), if higher-order dispersive effects are neglected.

The stationary GNSE (29) with boundary conditions (30)– (32) will be investigated further by the approximate variational method and numerically both in the anomalous (see Sec. III) and normal (see Sec. IV) dispersive regimes.

III. SOLUTIONS OF GNSE IN THE ANOMALOUS DISPERSIVE REGIME

A. Variational approach

In order to gain a deeper insight into properties of stationary solutions of GNSE (3) we introduce a simple semianalytical variational analysis. Most investigations (see, e.g., Refs. [41,42]), based on the direct variational approach, have used a trial function of the form

$$\Psi(r,t)=h(t)f(r/a(t))e^{\mathrm{i}b(t)W(r/a(t))+\mathrm{i}\Phi(t)+\mathrm{i}m\varphi},$$

where the amplitude h, beam width a, phase front curvature parameter (or chirp parameter) b, phase Φ, amplitude profile f, and phase profile W are real functions. The dynamical

equations that describe the evolution in time of soliton or vortex parameters have been obtained after the Ritz optimization in Ref. [34] for GNSE (3). The serious shortcoming of this approach is that the radial profile of the trial function is fixed. Therefore, such analysis is unable to account for the wave packet shape modification with energy (number of quanta N), which occurs to be essential for GNSE (3).

We restrict our variational analysis to the lowest-order solitonlike solutions ($m=0$) of the form $\Psi(r,t)=\psi_0(r)e^{i\Lambda t}$ with zero momentum and angular momentum. Such solutions are stationary points of the Hamiltonian at constant number of quanta. In our treatment we will take a proper account of the possible changing of the radial profile $\psi_0(r)$ with the number of quanta N. Previously, the variational problem, involving the super-Gaussian ansatz, was solved in Ref. [27] for GNSE (3) at $P=0$ and $DB>0$, showing very good agreement with numerical results. We are interested here rather in an analytically tractable analysis, which reveals physical reasons for soliton shape modification, than in a more precise description of a soliton profile.

One of the simplest appropriate trial functions for a localized solitonlike solution, satisfying boundary conditions (30) and (32), is

$$\psi_0(r)=\{h_1+h_2\mu^2r^2\}e^{-(1/2)\mu^2r^2}=\mu\sqrt{\frac{N}{2\pi}}f(\xi), \quad (35)$$

where $\xi=\mu r$. As is seen from Eq. (34), in the case $DP<0$ and $-D^2/(4P)<\Lambda<0$, the soliton has no oscillating tails ($\mathrm{Re}k=0$). Furthermore, if $\Lambda<-D^2/(4P)$, the soliton solution decreases at $r\to\infty$ rather rapidly, not slower than the decay rate $\mathrm{Im}k\geqslant\sqrt{|D/(2P)|}$. Therefore, a possible changing of the Gaussian-like soliton shape in the vicinity of the center ($r=0$) may be approximately described by a square function $h_1+h_2\xi^2$. The soliton amplitude at the center $h_1=\psi_0(0)$ can be expressed through N and h_2 with the help of the normalization condition (4):

$$(h_1+h_2)^2+h_2^2=\frac{N}{\pi}\mu^2.$$

The accuracy of the variational approach with the trial function (35) will be proved by numerical simulations (see below), even for solutions with nonlinear frequency shifts close to $\Lambda\approx0$, when their decay rates vanish ($\mathrm{Im}k\approx0$).

One of the advantages of the trial function (35) with $h_2>0$ (in comparison, for example, with the super-Gaussian ansatz [27]) is that it explains an appearance of a local minimum at the center of a soliton with sufficiently large N. Such ''hatlike'' shape solitons have been discovered numerically [see Figs. 1(a) and 1(b)].

Substituting the function (35) into Hamiltonian (7), we obtain

$$H=N\mu^2\{DI_d(\beta)-\mu^2PI_p(\beta)-NBI_b(\beta)-N^2\mu^2KI_k(\beta)\}, \quad (36)$$

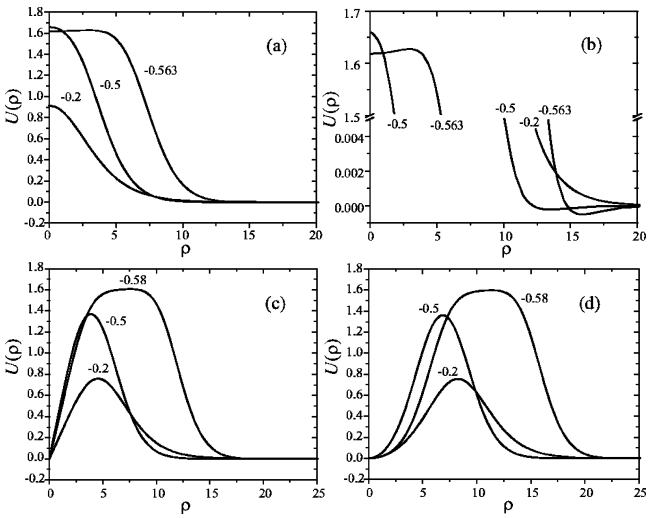

FIG. 1. Stationary solutions of GNSE in anomalous dispersive regime ($\kappa=0.3$): (a) solitons ($m=0$), (b) asymptotic behavior of the solitons near their centers and at large ρ, (c) vortices ($m=1$), (d) vortices ($m=2$). Values of nonlinear frequency shifts λ are indicated near the curves.

where μ is the first variational parameter, $\beta=h_2/(\mu\sqrt{N})>0$ is the second variational parameter, and the following definitions are used:

$$I_d(\beta)=\int_0^\infty[f'(\xi)]^2\xi d\xi,$$

$$I_p(\beta)=\int_0^\infty\left\{f''(\xi)+\frac{1}{\xi}f'(\xi)\right\}^2\xi d\xi,$$

$$I_b(\beta)=\frac{1}{2(2\pi)}\int_0^\infty f^4(\xi)\xi d\xi,$$

$$I_k(\beta)=\frac{1}{3(2\pi)^2}\int_0^\infty f^6(\xi)\xi d\xi.$$

As indicated above, the soliton corresponds to a stationary point of the Hamiltonian, provided that $N=\mathrm{const}$. Thus, a solution of the set of equations

$$\frac{\partial H}{\partial\mu}=0, \quad \frac{\partial H}{\partial\beta}=0 \quad (37)$$

determines soliton parameters μ_0 and β_0. The equation for β_0 may be written in the form

$$F(\beta_0)=0, \quad (38)$$

where

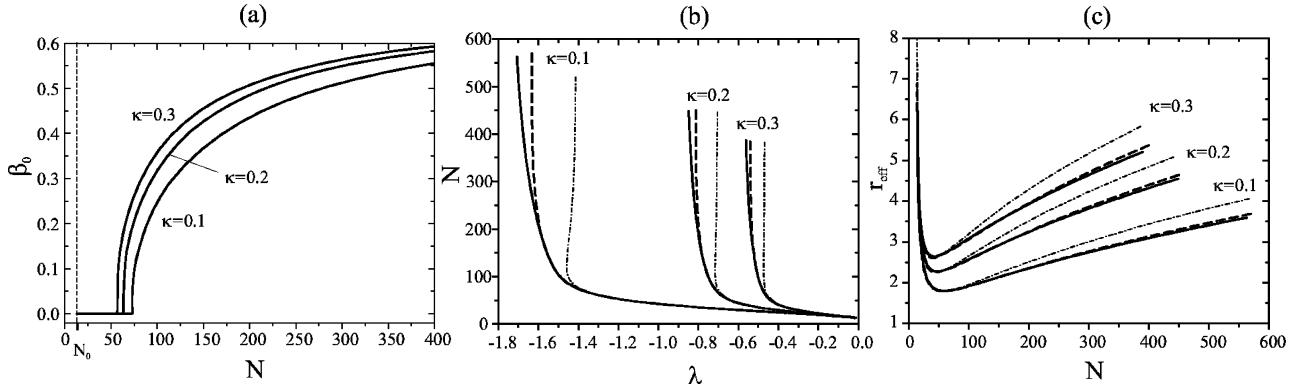

FIG. 2. Soliton solutions of GNSE in anomalous dispersive regime with different κ: (a) variational parameter β_0 vs number of quanta N ($\beta_0=0$ corresponds to Gaussian profile), (b) number of quanta vs nonlinear frequency shift, (c) effective width vs number of quanta. Solid curves for numerical results; dashed curves for results obtained by variational analysis with a trial function, which takes into account change of soliton shape; dot-dashed curves for results with trial function with unchanged Gaussian profile.

$$F(\beta)=2F_{pk}\frac{\partial F_{db}}{\partial\beta}-F_{db}\frac{\partial F_{pk}}{\partial\beta},$$

$$F_{pk}(\beta)=[PI_p(\beta)+N^2KI_k(\beta)],$$

$$F_{db}(\beta)=[DI_d(\beta)-NBI_b(\beta)]. \tag{39}$$

The variational parameter μ_0 is given by the expression

$$\mu_0^2=\frac{DI_d(\beta_0)-NBI_b(\beta_0)}{2[PI_p(\beta_0)+N^2KI_k(\beta_0)]}. \tag{40}$$

A stable soliton corresponds to the minimum or to the maximum of the Hamiltonian. Actually, if the function $\psi_0(r;\mu_0,\beta_0)$ realizes the extremum of the Hamiltonian (36) at the point (μ_0,β_0), then any deviation from this point in the plane (μ,β) leads to a change of H, which is impossible because of its conservation [43]. Hence, the soliton stability criterion coincides with the condition that the Hamiltonian reaches its minimum or maximum at the point $\mu=\mu_0$, $\beta=\beta_0$:

$$h=\left\{\frac{\partial^2H}{\partial\mu^2}\frac{\partial^2H}{\partial\beta^2}-\left(\frac{\partial^2H}{\partial\beta\partial\mu}\right)^2\right\}_{\mu=\mu_0,\ \beta=\beta_0}$$

$$=-4\mu_0^4N^2\left.\frac{\partial F}{\partial\beta}\right|_{\beta=\beta_0}>0, \tag{41}$$

where $F(\beta)$ is given by the expression (39). If the Gessian h is negative, then $\mu=\mu_0$, $\beta=\beta_0$ is a saddle point of the Hamiltonian, which corresponds to an unstable soliton solution. Therefore, in the framework of the variational approach, the stable solitonlike solution of GNSE in the anomalous dispersive regime is described by the function (35) with parameters μ_0, β_0, provided that β_0 satisfies the stability condition

$$\left.\frac{\partial F}{\partial\beta}\right|_{\beta=\beta_0}<0. \tag{42}$$

Let us consider how soliton features vary depending on the number of quanta. It is convenient to investigate the N dependence of soliton parameters β_0 and μ_0 at a fixed combination $\kappa=(K/P)/(B/D)^2$ of GNSE coefficients. The point is that after a proper time and space variable rescaling, a solution of stationary GNSE (29) will depend only on two parameters: nonlinear frequency shift and κ (see Sec. III B for details). The parameter β_0 versus N is plotted in Fig. 2(a) for GNSE with different κ.

It follows from Eq. (40) that the soliton solution of the GNSE in the regime (8) exists only if the number of quanta exceeds the threshold value $N_0=(|D|/|B|)[I_d(0)/I_b(0)]=4\pi D/B$. Indeed, $\mu_0^2(N)<0$ for $N<N_0$, which is impossible [remember that $B<0$ and $D<0$ in the regime (8)]. We have obtained this well known result (see, e.g., Ref. [42]) with the trial function (35), which has a Gaussian profile for solitons with a small number of quanta ($\beta_0=0$ if $N\approx N_0$). The threshold N_0 does not depend on coefficients P and K because $\mu_0(N)\to 0$ at $N\to N_0$ and higher-order corrections, proportional to P and K, become less significant. But, contrary to the case $P=K=0$, in the regime (8) there exist stable soliton solutions for $N>N_0$ if at least one of the coefficients P or K is not equal to zero.

Under the influence of focusing cubic nonlinearity, the soliton effective width (14) decreases, and the soliton amplitude increases correspondingly, while its number of quanta is growing close to the threshold N_0. However, along with that, the role of the higher-order dispersive term and defocusing quintic nonlinearity becomes more and more essential. An important feature of cubic-quintic nonlinear media is an existence of the self-defocusing regime, when the effective soliton width increases with N above some value N_f [see Fig. 2(c)]. One can easily find from Eq. (40) that the minimum of $r_{\rm eff}^2(N)\sim 1/\mu_0^2$ corresponds to $N=N_f$, where

$$N_f=N_0\left\{1+\sqrt{1+\frac{PI_p(0)}{KI_k(0)}\frac{[BI_b(0)]^2}{[DI_d(0)]^2}}\right\}$$

$$=N_0(1+\sqrt{1+8/(9\kappa)}), \tag{43}$$

and N_0 is the threshold for soliton existence. It is seen from

Eq. (43) that the number of quanta N_f, necessary to switch regimes from the self-focusing to self-defocusing one, is a decreasing function of parameter κ. In the limiting case $P \to 0$ ($\kappa \to \infty$), one obtains $N_f = 2N_0$. Note that even in the strongly nonlinear regime, the soliton profile is still Gaussian-like ($\beta_0 = 0$).

A soliton solution with unchanged Gaussian-like shape is stable if $N_0 < N < N_*$, where N_* is defined from equation $(\partial F/\partial\beta)_{\beta=0} = 0$, or

$$\frac{1}{\kappa} + \frac{32N_*^2}{27N_0^2}\left(1 - \frac{N_*}{4N_0}\right) = 0. \tag{44}$$

At $N = N_*$ the derivative $(\partial F/\partial\beta)_{\beta_0=0}$ [which, in accordance with criterion (41), determines the stability of a soliton] changes its sign. The solution with $\beta_0 = 0$ becomes unstable if $N > N_*$, but a new stable soliton appears with $\beta_0 > 0$. The value of parameter β_0 sharply increases, and the soliton's shape becomes more and more flattened with the rise of the number of quanta above N_*. The radial profile $\psi_0(r)$ even yields a local minimum at $r = 0$ above some other critical value of $N > N_*$. Note that the Gessian (41) is equal to zero at $N = N_*$, hence N_* corresponds to the bifurcation point of the Hamiltonian (36). The fact that soliton parameters abruptly change when the number of quanta exceeds the bifurcation point N_* corroborates an interesting conception [42] of phase transition or ''light condensation'' in nonlinear optical materials with cubic-quintic nonlinearity. The authors of Ref. [42] revealed a surprising similarity between light condensates (laser beams with power $N > N_*$) and liquids. By numerical simulations of soliton collisions against planar boundaries and localized inhomogeneities, they demonstrated that 2D ''liquid solitons'' behave like liquid droplets having a surface tension. As follows from Eq. (44), the critical value N_* is a decreasing function of κ. In particular, $N_* = 16\pi D/B = 4N_0$ in the limiting case $P \to 0$ or $\kappa \to \infty$. It coincides with the critical point of the phase transition obtained in Ref. [42] by the frequency spectrum analysis of the small amplitude oscillations of the perturbed stationary soliton solution. However, the condition for such a phase transition may be changed significantly with regard to the higher-order dispersion, especially if $\kappa \ll 1$.

B. Numerical modeling of steady-state solutions

For numerical simulation it is useful to reduce the number of parameters of Eq. (29) using the following rescaling transformation: $r = \rho\sqrt{P/|D|}$, $\Lambda = \lambda D^2/P$, $\psi(r) = U(\rho)\sqrt{D^2/|B|P}$. We are looking for a solution of the form (28), assuming that the radial function $U(\rho)$ is real. Then Eq. (29) may be rewritten as

$$-\lambda U + \delta\Delta_\rho^{(m)}U + (\Delta_\rho^{(m)})^2 U - U^3 + \kappa U^5 = 0, \tag{45}$$

where $\delta = \mathrm{sgn}(D)$, $\kappa = (K/P)/(B/D)^2$. In this section we analyze two-parameter families (with parameters λ and κ) of solitonlike and vortexlike solutions of Eq. (45) for $\delta = -1$.

We have solved the boundary problem (45), (30)–(32) numerically by the relaxation method in spectral space, with the trial function of the variational analysis (employed in Ref. [34]) as the initial approximation. We have used the Hankel spectral transformation, which is equivalent to an expansion of the radial function $U(\rho)$ in Bessel functions $J_m(k\rho)$. It gives a very suitable spectral representation of Eq. (45) in polar coordinates. The stabilizing multiplier method [44] has been used in order to obtain a convergent iterative process.

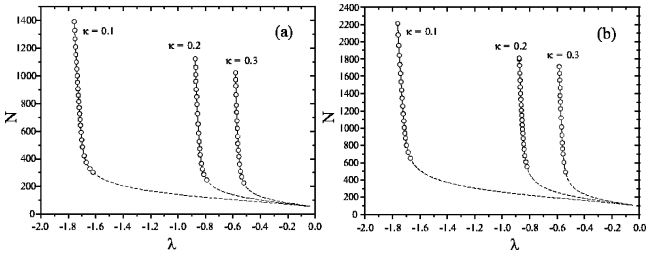

FIG. 3. Number of quanta vs nonlinear frequency shift for vortices in anomalous dispersive regime with different κ: (a) $m = 1$, (b) $m = 2$. Dashed curves for unstable vortices, curves with circles for stable vortices.

Numerically obtained radial profiles of solitonlike solutions ($m = 0$) are shown in Fig. 1. It is seen in Figs. 1(a) and 1(b) that the soliton shape over some critical value of N (very close to N_*, found in Sec. III A) drastically changes: it becomes flat topped. Above some higher value of N, a local minimum on the profile $U(\rho)$ appears at $\rho = 0$ [see Fig. 1(b)]. These features are in a qualitative correspondence with the variational analysis described in Sec. III A. As was pointed out in Sec. II B, solutions of GNSE (22) with $\Lambda < -D^2/(4P)$ (after rescaling $\lambda < -0.25$) have oscillating tails, and they are seen in Fig. 1(b). It follows from Eq. (26) that $\lambda > -0.25$ for all solutions of Eq. (45) with $\kappa > 27/32$. Therefore, only solutions asymptotic, monotonic at infinity, exist in this case. The radial profiles of vortices with topological charges $m = 1$ and $m = 2$ are presented in Figs. 1(c) and 1(d). The 2D intensity shape for vortices is of the ringlike form with the dark ''hole'' at the center. Vortices also change radial profiles if their numbers of quanta exceed some critical value N_{cr}, which is a decreasing function of κ. The value N_{cr} increases with topological charge m.

Let us compare energy-dispersion diagram (EDD): number of quanta (soliton energy) N versus nonlinear frequency shift λ and the N dependence of the soliton effective width $r_{\mathrm{eff}}(N)$, obtained numerically and by the variational method with different trial functions. Results with the ansatz (35), restricted by the single variational parameter μ ($h_2 \equiv 0$ or $\beta \equiv 0$), are given in Figs. 2(b) and 2(c) by dot-dashed curves, solid curves correspond to numerical solutions, dashed curves to the variational approach with a trial function that can change a profile, having two variational parameters μ and β. The EDD for solitonlike ($m = 0$) and vortexlike solutions (with $m = 1$ and $m = 2$) of Eq. (45) at different κ are presented in Fig. 2(b) and in Figs. 3(a) and 3(b), respectively. To excite a structure with topological charge m, one must exceed some threshold value N_m for the number of quanta, which corresponds to the gap of $N(\lambda)$ at $\lambda \to 0$. The threshold value N_m increases with topological charge m. We have

obtained numerically the following threshold values: $N_0 \approx 12$ (variational approach of Sec. III A predicts $N_0 = 4\pi$), $N_1 \approx 47$, $N_2 \approx 88$. Figure 2(c) presents the N dependence of the effective soliton width r_{eff}, determined by expression (14). As was predicted in Sec. III A, $r_{\text{eff}} \to \infty$ at $N \to N_0$, since, according to Eq. (40), $\mu_0(N_0) = 0$. Note that the soliton shape begins to change noticeably in the self-defocusing regime [see Figs. 1(a), 1(b), and 2].

Thus, our variational analysis with the trial function (35) gives a good description both of the effective soliton width $r_{\text{eff}}(N)$ and of the $N(\lambda)$ diagram [see Figs. 2(b) and 2(c)]. A rather good quantitative correspondence of the variational analysis with numerical results for large number of quanta $N > N_*$ is achieved only by taking into account the change of soliton profile.

However, one cannot study the stability of solitons and vortices with respect to radially asymmetric perturbations in the framework of any variational approach with a radially symmetric trial function. Stability conditions of steady-state solutions, regarding small general 2D perturbations, may be obtained by a linear stability analysis.

C. Linear stability analysis

It is very important for many applications to verify whether steady-state solutions are stable. For GNSE (3) with $P = 0$ in the anomalous dispersive regime, it was found previously that solitons are robust, but vortices may be stable against small radially symmetric perturbations and unstable against azimuthal perturbations. As a result of instability, a vortex breaks up into several solitons, which fly off tangentially to the initial ring, conserving the total angular momentum (5). Such behavior was considered as a consequence of modulational instability (see, e.g., Refs. [45,46]). However, detailed recent investigations [47,48] have shown that stable one-charged ($m = 1$) and two-charged ($m = 2$) vortex solutions of the cubic-quintic GNSE with $P = 0$ do exist in the self-defocusing regime. Nevertheless, the complete suppression of vortex symmetry-breaking instability is not explained yet. It is remarkable that even 3D completely stable vortices have been recently theoretically discovered in cubic-quintic nonlinear media [49] and also in the media with quadratic nonlinearity combined with self-defocusing cubic nonlinearity [50]. This gives rise to the view [50] that the stability property of vortices with large enough energy (number of quanta) is a universal feature of the media with competing nonlinearities.

Evidently, a thorough examination of soliton and vortex stability is needed also in the case under consideration when $P \neq 0$. We will start an investigation of their stability by a linear analysis of the dynamics of small perturbations, which are taken as a superposition of azimuthal Fourier modes (similar to the analysis in Refs. [45,47–50]). Let us consider some stationary solution of GNSE (3) of the form (28), which is perturbed radially and azimuthally:

$$\Psi(\mathbf{r},t) = \{\psi(r) + a^+(r,t)e^{iL\varphi} + a^-(r,t)e^{-iL\varphi}\} \times \exp\{im\varphi + i\Lambda t\}, \tag{46}$$

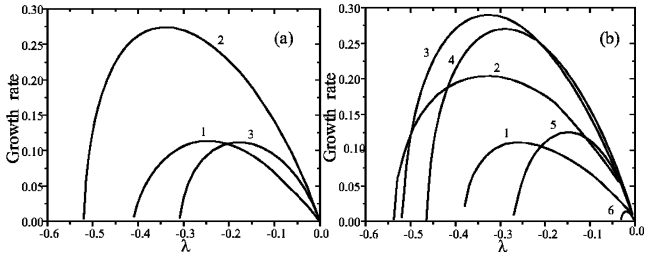

FIG. 4. Maximum growth rates of all unstable azimuthal eigenmodes vs nonlinear frequency shift for vortex solutions in anomalous dispersive regime ($\kappa = 0.3$): (a) $m = 1$, (b) $m = 2$. Integers near the curves indicate azimuthal numbers L.

where $L = 0, 1, 2, \ldots$ is the azimuthal number of perturbation. Substituting Eq. (46) in Eq. (3) and neglecting nonlinear (with respect to $a^{\pm}$) terms, we obtain the set of two complex equations generalizing the set, obtained in Ref. [47], to the case of the GNSE with $P \neq 0$:

$$\left(i\frac{\partial}{\partial t} + \hat{Q}^{\pm}\right)a^{\pm}(r,t) + q(r)[a^{\mp}(r,t)]^* = 0, \tag{47}$$

where

$$\hat{Q}^{\pm} = -\Lambda + D\Delta_r^{(m\pm L)} + P(\Delta_r^{(m\pm L)})^2 + 2B|\psi|^2 + 3K|\psi|^4,$$

$$q(r) = B|\psi|^2 + 2K|\psi|^2\psi^2.$$

Unstable perturbations are supposed to be localized in space, growing exponentially with time: $a^{\pm} \sim e^{\Gamma_L t}$. Thus, the growth rate Γ_L can be obtained as a solution of the eigenvalue problem. We have solved this problem numerically in Hankel spectral space.

Solitons have been found to be stable with respect to modulational instability: growth rates for any L are equal to zero. However, the vortex is unstable if its number of quanta is below some critical value N_{cr}. The maximum growth rates of all unstable eigenmodes for vortices with $m = 1$ and $m = 2$, as functions of nonlinear frequency shift λ, are presented in Fig. 4. Integers near the curves $\Gamma_L(\lambda)$ correspond to azimuthal numbers L. Radially symmetric perturbation (mode $L = 0$) has zero growth rate. For a one-charged vortex ($m = 1$), we have found that only azimuthal modes with L, falling in the interval $1 \leqslant L \leqslant L_{\max} = 3$, are unstable. For the two-charged vortex ($m = 2$), the maximum azimuthal number $L_{\max}$ of the unstable mode is equal to 6. The largest growth rate corresponds to the mode with median number L. All unstable modes have nonzero growth rates at least in a small vicinity of the threshold N_m, which corresponds to $\lambda \approx 0$. Note, that small-scaled perturbations (with the largest L) are completely suppressed even for the number of quanta close to the threshold. A perturbation with the azimuthal number $L = 2$ has always the widest instability region. It is that mode which defines the edge of the stability region. If $\kappa \neq 0$, there are stable vortices with number of quanta above the critical values N_{cr}, for which modulational instability is completely suppressed. Similar to the critical number of quanta N_* for solitons, N_{cr} increases as parameter κ de-

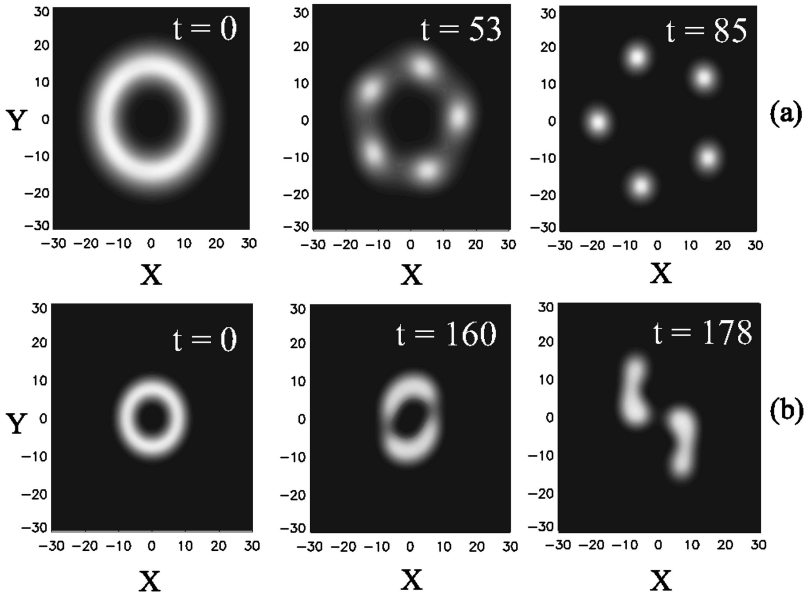

FIG. 5. Spatial-temporal evolution of intensity distribution of unstable vortex solution in anomalous dispersive regime ($m=2$, $\kappa=0.3$): (a) $\lambda=-0.05$, (b) $\lambda=-0.54$ (close to the edge of unstable region) vortex decays into two-hump structures.

creases, and $N_{\rm cr}\to\infty$ in the limiting case $K\to 0$. Thus, the growth rates are monotonically increasing functions of N, i.e., vortex solutions of GNSE (3) with $K=0$, $P\neq 0$ are always unstable.

Obviously, the linear stability analysis is unable to describe the nonlinear evolution of unstable vortices. But it is natural to suppose that, due to the development of modulational instability against perturbation with azimuthal period $T=2\pi/L$, the vortex would break up into L stable solitons, where $1\leqslant L\leqslant L_{\max}$. The origin of the upper limit on the number of appearing solitons is quite clear. During evolution, any localized structure must conserve its number of quanta N. To excite L solitons, one should at least exceed the threshold value: $N\geqslant LN_0$, where N_0 is the threshold for a single stable soliton excitation. Since an instability region for the mode with largest number L is concentrated in the neighborhood of $\lambda\approx 0$ (or $N\approx N_m$), the number $L_{\max}$ can be estimated as the ratio of the thresholds for the vortex N_m and for the soliton N_0:

$$L_{\max}\leqslant\left[\frac{N_m}{N_0}\right], \tag{48}$$

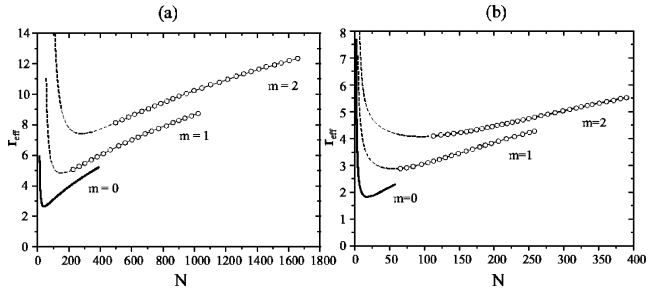

FIG. 6. Effective widths of localized structures in different dispersive regimes vs number of quanta ($\kappa=0.3$). Numerical results: (a) anomalous dispersive regime, (b) normal dispersive regime. Solid curves for solitons, dashed curves for unstable vortices, curves with circles for stable vortices.

where square brackets $[f]$ mean the integer part of f. Relation (48) gives the upper estimate for the number of solitons that can appear, because some portion of energy (number of quanta) of the unstable vortex can be carried out by free waves.

Thus, the linear stability analysis gave us the sufficient conditions of instability and revealed the region of the number of quanta where vortex solutions are stable. On the basis of obtained results, we predict a possible fission scenario for unstable vortices.

Strictly speaking, to study the stability of solitons and vortices with respect to finite 2D perturbations, a nonlinear spatial-temporal problem should be solved. This is the aim of the following section.

D. Numerical simulation of the nonstationary GNSE

All results about the stability of solitons and vortices have been verified by simulations of the nonstationary GNSE (3) with perturbed steady-state solutions as initial conditions. In numerical investigations, most authors modeled random physical inhomogeneities by imposing an asymmetric perturbation (for example, Gaussian noise [45]) on a stationary solution. However, in the experimental setup, some kind of symmetric artificial obstacles can be purposely mounted in the path of the wave beam in order to influence on the dynamics of the unstable vortex. Because of this, we have investigated how different types of finite perturbations—radially symmetric, azimuthally periodical [as in linear analysis, see Eq. (46)], and general asymmetric ones—influence the evolution of perturbed stationary solutions of the GNSE.

For simulation of nonstationary GNSE (3), the split-step Fourier transform method (see, e.g., Ref. [11]) with monitoring of conservation of integrals (4)–(7) has been used.

Simulations mainly confirm even quantitative predictions, given by linear analysis. Solitons have been found to be stable in the whole region where they exist. Vortices are unstable with respect to the modulational instability in the re-

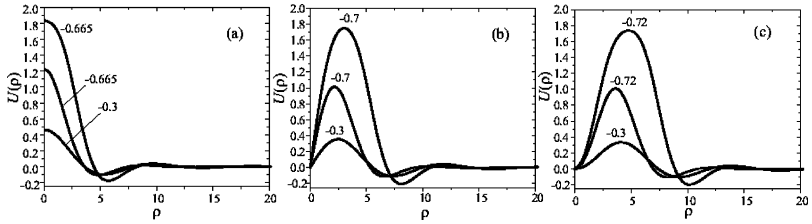

FIG. 7. Stationary solutions of GNSE in normal dispersive regime ($\kappa=0.3$) for different nonlinear frequency shifts λ: (a) solitons ($m=0$), (b) vortices ($m=1$), (c) vortices ($m=2$).

gion of diagram $N(\lambda)$, predicted by linear analysis. If a perturbation with azimuthal number L is imposed on steady vortices and they have nonzero growth rates $\Gamma_L(N)$, then it necessarily grows up in numerical simulations. But linear analysis describes only an initial stage of instability. Nonlinear dynamics of unstable vortices in the general case is very intricate. If the growth rate of the perturbation is small but nonzero $[0<\Gamma_L(N)\ll 1]$ and the perturbation has azimuthal period $T=2\pi/L$, then L filaments begin to develop. But we have observed that in the process of unstable vortex evolution, some filaments may fuse or break into pieces and so the final number of solitons that fly away may be not equal to L. We have found that, if a radially symmetric, asymmetric, or periodical perturbation with azimuthal number $L>L_{\max}$ is imposed, then the vortex with number of quanta $N<N_{\rm cr}$ finally breaks up too. The number of filaments in this case, as a rule, corresponds to the azimuthal mode with the maximum growth rate for given N. In all probability, the vortex chooses unstable modes from the spectrum of imposed asymmetric perturbation or from numerical noise. The perturbation with the largest growth rate develops faster and usually dominates. Nevertheless, in most cases one can *control* the number of appearing solitons by imposing perturbation with a definite azimuthal period on the unstable vortex.

Typical examples, illustrating the spatial-temporal evolution of intensity distribution of unstable vortices with topological charge $m=2$, are shown in Fig. 5. Figure 5(a) represents the dynamics of the vortex from the middle of unstable region with a perturbation $L=5$. Figure 5(b) represents an interesting dynamics of two-hump structures, which sometimes appear at the edge of the unstable region of diagram $N(\lambda)$. These structures fly away just after formation, each of them revolves on its axis, and peaks of the intensity periodically flow from one hump to another. It was found in numerical simulations that a *nearly stable* vortex with number of quanta $N\approx N_{\rm cr}$ always breaks up into two fragments. However, sometimes each of the appearing filaments finally decays into several solitons and free waves.

The dynamics of perturbed solitons and perturbed stable vortices is found to be quasiperiodic. The effective width and amplitude of a stable structure oscillate. Near the unstable region the amplitude of oscillations can be rather large, but a stable vortex still survives. Performing long-term numerical simulations (duration of over hundred typical oscillation periods), we have confirmed the main result of our linear analysis about the stability of vortices with number of quanta above some critical value $N_{\rm cr}$.

Thus, though in the framework of GNSE (3) with the fourth-order dispersive term and Kerr-type nonlinearity ($K=0$) in the anomalous dispersive regime (8) stable solitons do exist, vortices are unstable in this case. Vortex may be stable only in the self-defocusing regime when its effective width increases with the number of quanta [see Fig. 6(a)]. For our model, this regime is realized under the influence of a saturable cubic-quintic nonlinearity ($BK<0$). Moreover, even in the self-defocusing regime, the vortex becomes stable only above some critical number of quanta $N_{\rm cr}$, when its radial profile is flattened.

IV. SOLUTIONS OF GNSE IN THE NORMAL DISPERSIVE REGIME

A. Variational approach

In this section we consider only solitonlike solutions with topological charge $m=0$ by means of the procedure described above. We choose the trial function in the form of the

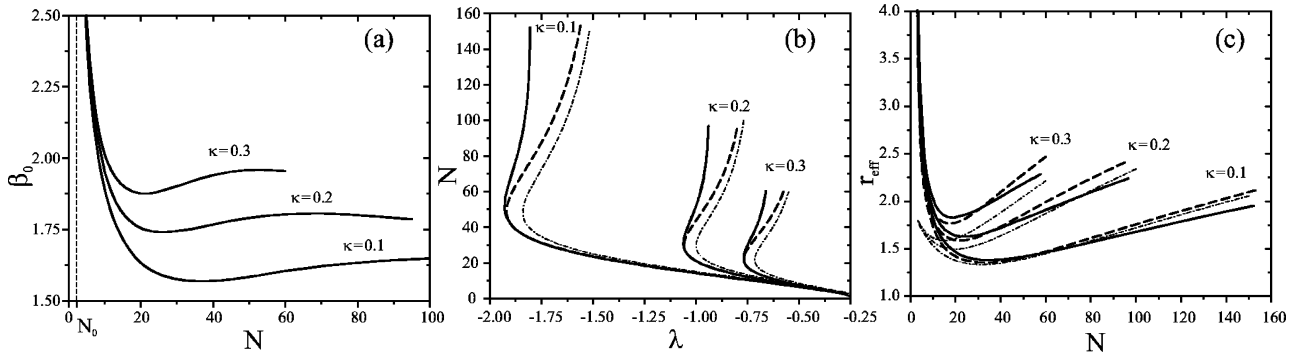

FIG. 8. Soliton solution of GNSE in normal dispersive regime with different κ: (a) variational parameter β_0—number of soliton oscillations on characteristic soliton width ($\sim 1/\mu_0$) vs number of quanta, (b) number of quanta vs nonlinear frequency shift, (c) effective width vs number of quanta. Solid curves for numerical results; dashed curves for results obtained by variational analysis with a trial function, which takes into account soliton oscillations; dot-dashed curves for trial function with Gaussian profile.

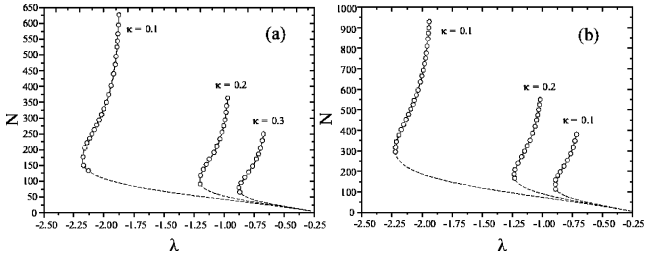

FIG. 9. Number of quanta vs nonlinear frequency shift for vortex solutions of GNSE in normal dispersive regime with different κ: (a) $m=1$, (b) $m=2$. Dashed curves for unstable vortices, curves with circles for stable vortices.

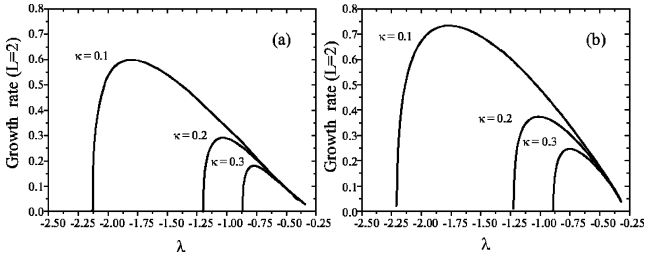

FIG. 10. Maximum growth rates of eigenmodes with the widest unstable region, corresponding to mode with azimuthal number $L=2$, for vortex solutions in normal dispersive regime at different κ: (a) vortices $m=1$, (b) vortices $m=2$.

product of two functions as in Sec. III A. One of them (Gaussian-like) mainly describes the spatial localization of a soliton. But the choice of the second function is not so straightforward as it was for GNSE with $DP<0$, regime (8). According to the analysis of the linear asymptotic of GNSE with $DP>0$ (see Sec. II B), localized stationary solutions oscillate and slowly decay at infinity, especially if $\Lambda \approx -D^2/(4P)$. Thus, to obtain the proper trial function, for all possible Λ, one should accurately take into account the linear asymptotic of the solution. Since the Bessel function $J_0(\gamma r)$ is an eigenfunction of linear operators $\Delta_r^{(0)}$ and $(\Delta_r^{(0)})^2$, the suitable trial function for a localized solitonlike solution is supposed to be

$$\psi_0(r) = hJ_0(\gamma r)e^{-(1/2)\mu^2 r^2} = \mu\sqrt{\frac{N}{2\pi}}f(\xi;\beta), \qquad (49)$$

where the normalized function $f(\xi;\beta)$ depends on the variable $\xi=\mu r$ and parameter $\beta=\gamma/\mu$. The normalizing factor h can be expressed through N, using the definition (4). The first variational parameter μ mainly characterizes the soliton width. The second one, namely, $\beta=\gamma/\mu$ characterizes the number of oscillations on the characteristic soliton width $\sim\mu^{-1}$. Formulas determine soliton parameters μ_0 and β_0 remain the same as in Sec. III A (except for changing of the sign of coefficient D and values of integrals) and are given by Eqs. (40) and (38) and Eq. (42), respectively.

An existence of the threshold number of quanta for soliton excitation is not so obvious now from formula (40) as in Sec. III A, because in the case under consideration, all terms in this formula are positive. However, one can show that μ_0 tends to zero when N tends to the finite threshold value N_0. To show this, let us note that, according to expression (34), $\mathrm{Re}k \approx \sqrt{D/(2P)} \gg \mathrm{Im}k$ near the largest possible value of the nonlinear frequency shift $\Lambda=-D^2/(4P)$, and so the oscillating nature of the soliton solution becomes essential. The spatial frequency of oscillations, γ, remains finite when the parameter μ_0, characterizing decay rate, tends to zero, so that parameter $\beta_0=\gamma/\mu_0$ simultaneously tends to infinity [see Fig. 8(a)]. Therefore, the threshold value of N for soliton existence may be determined at the limit $\beta_0\to\infty$. This limit may be found from Eq. (38). It is easy to see that the threshold value N_0 does not depend on K, because the integral $I_k(\beta_0)$ tends to infinity for $\beta_0\to\infty$ slower than the integral $I_p(\beta_0)$. One can finally find that $N_0=C_0|D|/|B|$, where

$$C_0 = \lim_{\beta_0\to\infty}\frac{2I_pI_d' - I_p'I_d}{I_p'I_d - 2I_pI_d'} \approx 2.2.$$

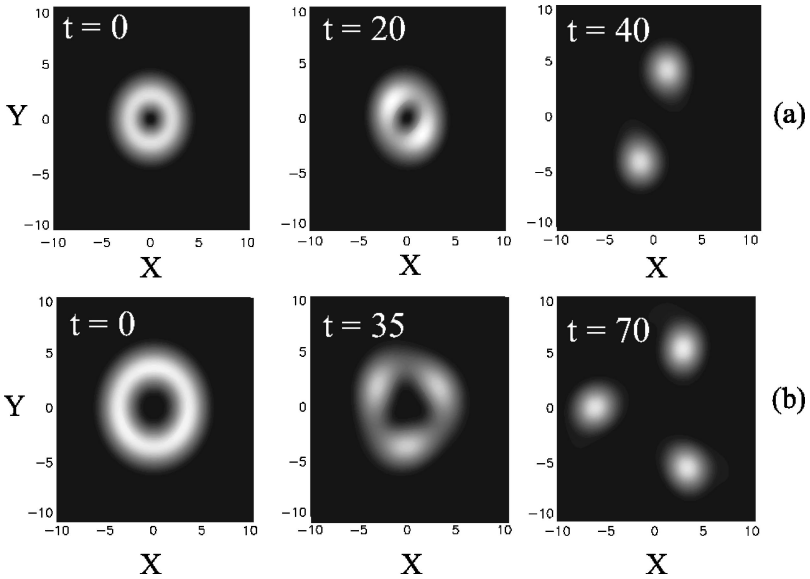

FIG. 11. Spatial-temporal evolution of intensity distribution of unstable vortex solutions in normal dispersive regime ($\lambda=-0.75$, $\kappa=0.3$): (a) $m=1$, (b) $m=2$.

Note that the threshold value N_0 is much lower than it was in the regime of anomalous dispersion (coefficient C_0, found by the variational analysis of Sec. III A, was equal to 4π).

The accuracy of variational analysis in determining the threshold value N_0 for existence of solitons and their stability is confirmed by our numerical calculations (see Sec. IV B for details). Figures 8(b) and 8(c) represent the EDD and N dependence of the effective width for soliton solution ($m=0$). One can see from Fig. 8(b) that variational and numerical approaches for the EDD fit each other much better in the case when soliton profile oscillations are taken into account in the trial function. The threshold value N_0 corresponds to $\Lambda=-D^2/(4P)$ or $\lambda=-0.25$ on this figure. Variational analysis predicts *bistability* of solitons in the normal dispersive regime—coexistence of two stable solutions with different number of quanta but with equal nonlinear frequency shifts. Figure 8(c) represents effective soliton width as a function of number of quanta, obtained numerically and by variational analysis. Note, that the trial function (49), which does not take into account oscillations ($\gamma=0$) is not able to reproduce asymptotic behavior of soliton width at $N\to N_0$ even qualitatively. We conclude that our variational approach with the trial function that correctly describes the linear asymptotic of the solutions gives qualitatively appropriate description of the EDD [Fig. 8(b)] and of the N dependence of the effective soliton width [Fig. 8(c)].

B. Numerical modeling

Numerical soliton and m-charged vortex solutions of Eq. (45), with boundary conditions (30)–(32) at $\delta=1$ and at different λ are presented in Fig. 7. The profiles with equal λ (but different N) illustrate the coexistence of solutions from the lower and upper branches of diagram $N(\lambda)$ [see also Fig. 8(b) and Fig. 9]. It is seen in Fig. 7 that closer to the edge of the region, where localized solutions exist [in the regime (8) it corresponds to $\lambda\approx-0.25$], their oscillating tails become more pronounced.

Figure 9 represents the EDD for vortices with $m=1$ and $m=2$. The nonlinear frequency shift for a localized solution in the normal dispersive regime is bounded from above, $\lambda<-0.25$, as was pointed out in Sec. II B. The threshold values N_m—number of quanta necessary to excite a soliton ($m=0$) or vortex ($m\neq 0$)—are less than the corresponding thresholds for the GNSE in the anomalous dispersive regime, which were indicated in Sec. III B. The values N_m increase with the topological charge m. In the case under consideration [regime (9)] we have found numerically the following threshold values: $N_0\approx 2.15$, $N_1\approx 4.5$, $N_2\approx 6.6$.

As in Sec. III C, we have investigated the stability of obtained solutions by linear analysis. The radially symmetric mode ($L=0$) is found to have a zero growth rate for any soliton or vortex solutions. Solitons are found to be stable also with respect to any perturbations with $L\neq 0$. But vortices can break up because of modulational instability. Azimuthal perturbation with $L=2$ has the widest instability region, as before (see Sec. III C). Therefore, a suppression of the modulational instability of the mode with $L=2$ leads to a complete stability of the vortex in the framework of linear stability analysis. Figure 10 represents the maximum growth rates for this most dangerous mode. Note, that the instability region becomes wider for lower values of coefficient κ. As it was for the anomalous dispersive regime (8), GNSE (3) in the case $K=0$ has only unstable vortexlike solutions, and their growth rates increase monotonically with N. It is connected with the fact that in the absence of a saturable nonlinearity ($K=0$), there is no self-defocusing regime ($dr_{\mathrm{eff}}/dN<0$ for all N) for the solutions of Eq. (3). We have found that only perturbations with azimuthal numbers $L=1,2\ldots,L_{\max}$ have nonzero growth rates. For vortices with topological charge $m=1$ we have obtained $L_{\max}=2$, and $L_{\max}=3$ for vortices with $m=2$. The value $L_{\max}$ gives an upper estimate for the number of stable solitons, which may appear as a result of the modulational instability of a vortex with topological charge m. This number can be estimated also from Eq. (48).

All results, obtained in the linear approximation, have been verified by long-term simulations of Eq. (3) with perturbed steady-state solutions as initial conditions. Solitons have been found to be stable with respect to all investigated types of finite perturbations. The spatial-temporal evolution of localized structures in the normal dispersive regime is similar to that described in Sec. III D. In Fig. 11 we represent examples of unstable vortices breaking up into $L_{\max}$ stable solitons. Simulations confirm the existence of stable vortices with the number of quanta above some N_{cr} in the self-defocusing regime [see Fig. 6(b)]. The dynamics of stable perturbed structure is found to be quasiperiodic.

Thus, solitons and vortices in the framework of GNSE (3) with Kerr-type ($K=0$) and cubic-quintic nonlinearities in the normal dispersive regime do exist only if the fourth-order dispersive effect is taken into account. If $DP>0$, but $K=0$, there is no self-defocusing regime: the effective width of any localized structure is a monotonically decreasing function of N, in this case only solitons occur stable. As for vortices, they are stable in the normal dispersive regime only under a *combined* influence of higher-order dispersion and quintic nonlinearity.

V. DISCUSSION AND APPLICATIONS

The main conclusion of our investigation is that in the framework of GNSE (3) with fourth-order dispersion and cubic-quintic nonlinearity, stable solitonlike and vortexlike structures can exist both in anomalous [Eq. (8)] and normal [Eq. (9)] dispersive regimes.

Our model is relevant first of all to a problem of propagation of intensive electromagnetic waves in magnetized plasmas. These waves may have rather complicated dispersive and polarization properties. Especially, it concerns whistler waves, which exist in a wide frequency range from ion plasma frequency to electron cyclotron frequency ω_{Be}. Whistlers (or helicons) are often observed in the ionosphere and magnetosphere of the Earth, in a laboratory gas plasma and in an electron plasma of solids. Properties of small amplitude whistler waves are well described by the theory, but many experimental observations of propagation of large amplitude whistler waves are not explained yet. In particular, it concerns an existence of stationary self-focusing not only in

anomalous but also in normal dispersive regimes [3,8]. We have shown above that solitons (or stationary waveguides) are robust against rather large symmetric and asymmetric perturbations, even in the Kerr nonlinear medium [Eq. (3) with $K=0$], if the fourth-order dispersion effect is taken into account ($P\neq 0$). Dispersive or polarization effects become very essential for whistlers with frequency close to $\omega_{Be}/2$, where the coefficient D in Eq. (3) vanishes (see the Appendix). We think that our model gives an appropriate qualitative explanation of these experiments. (See the Appendix for the derivation of the model equation for whistler wave self-focusing propagation and a comparison of our theoretical results with experiments.)

We have introduced simple variational analysis, which was found to be in very good agreement with our numerical simulations of solitons. In the normal dispersive regime, change of soliton parameters with the number of quanta has been correctly predicted by our variational approach, regarding the soliton profile oscillations in this regime. In the anomalous dispersive regime higher accuracy of variational results was achieved by means of the trial function, which takes into account the modification of the soliton shape with N. This provides an insight into the existence of some critical number of quanta N_* at which a soliton abruptly changes its radial profile. We have shown that the value N_* coincides with the point of gas-liquid phase transition, obtained in Ref. [42] for laser light in optical cubic-quintic media. We have found that this transition comes within the self-defocusing regime and have investigated an influence of the higher-order dispersive effect and quintic nonlinearity on soliton properties in both phase states.

Vortexlike envelope electromagnetic wave structures have not been discovered in plasmas yet. However, localized optical vortex structures have been observed in nonlinear optical materials and became a subject of many theoretical and experimental investigations. We have studied the influence of quintic nonlinearity and fourth-order dispersive effect on the properties and stability of vortices. Both in the anomalous and normal dispersive regimes, vortices can be stable only if their effective widths increase with N. But even in such a strongly nonlinear self-defocusing regime, vortices occur stable exceptionally above some critical value N_{cr} for the number of quanta. At the same time, in the normal dispersive regime bright robust vortices may exist only in the presence of higher-order dispersion ($P\neq 0$). Therefore, vortices in this regime may be stable only under the influence of both the effects considered in this paper: fourth-order dispersion ($P\neq 0$) and quintic nonlinearity ($K\neq 0$).

It was demonstrated numerically that vortex rapidly changes its shape if the number of quanta exceeds the critical number of quanta N_{cr} for vortex stability. Its profile becomes flat topped, similar to the radial profile of a soliton in a liquid phase state, when the number of quanta is above the critical point N_*. Therefore, it is reasonable to conclude that N_{cr} corresponds to the point of phase transition for a vortex. Using an analogy with fluid mechanics, one can say that only the liquid vortex becomes robust, because it has the effective surface tension strengthening such a vortex. If a vortex is unstable, it decays into solitons that fly away, conserving the total angular momentum of the system. Using the number of quanta conservation law, we have found the upper estimate for a number of stable solitons that can appear after fission of an unstable vortex.

As was pointed out in Ref. [16], the fourth-order dispersion effect may be of importance also in discrete molecular 2D systems: due to the nonlocal linear dispersion effect [20] and due to the next order approximation of linear 2D difference operators by differential operators in the quasicontinuum limit. Also it may describe competing short- and long-range dispersive interactions [22]. The quasicontinuum model for such a system was obtained in Ref. [22]. And then it was discussed on the basis of a simplified equation, which coincides with GNSE (3) in the particular case $D=K=0$. Taking into account the presence of some kind of saturable nonlinearity ($K\neq 0$), in the case $D=0$ it is possible to obtain not only stable soliton solutions but also stable vortices. As was shown above, it is also possible to extend a quasicontinuous analysis to the case where the second-order dispersion term does not vanish. In Ref. [22], soliton solutions have been found numerically on the basis of the discrete model in two qualitatively different regimes, which correspond to the anomalous and normal dispersive regimes, in our ''language.'' There is an interesting similarity between the results of our continuum model and the discrete model considered in Ref. [22], namely, between $N(\lambda)$ diagrams, dependence of the critical power N_0 on the linear dispersion parameter [corresponding to D in Eq. (3)], and in the form of solitons radial profiles, which may be monotonic or nonmonotonic (''staggered''), depending on the regime considered.

We believe that our investigation provides a broad spectrum of further applications in different physical systems, such as upper-hybrid 2D structures in magnetized plasmas, bright solitons and vortices in nonlinear optical media, Bose-Einstein condensates, and in 2D discrete molecular systems.

APPENDIX: STATIONARY WHISTLER WAVE BEAM PROPAGATION

Our model provides the theoretical background for an explanation of whistler wave propagation in self-induced waveguides, observed in the laboratory experiments carried out by Stenzel [3]. Above some threshold value of input high-frequency power, the strong density depression was formed first in the near-antenna region in these experiments. After some time it saturated into a long external magnetic-field-aligned density trough, in which the whistler wave was captured (ducted). This process was accompanied by a strong plasma electron heating. It is remarkable that the self-trapping into channels with depressed plasma density was observed at different values of pump frequency, *both in anomalous and in normal dispersive regimes* of whistler waves.

Here we obtain the model GNSE for nonlinear whistler wave beam stationary propagation in the direction of the external magnetic field $\mathbf{B}=B_0\mathbf{e}_z$, supposing that the main nonlinear effect is connected with Joule heating and with an extraction of plasma from regions of stronger plasma pres-

sure, caused by an increase of electron temperature in the strong wave field. The plane linear whistler wave, which obeys the dispersion relation

$$\omega(k)=\frac{c^2 k k_z \omega_{Be}}{\omega_{pe}^2+c^2k^2} \tag{A1}$$

(here ω_{pe} is the electron plasma frequency, $\omega_{pe}\gg\omega_{Be}$, $k=\sqrt{k_z^2+k_\perp^2}$), is an electromagnetic left-hand polarized wave, if it propagates along the magnetic field ($k_\perp=0$). However, a whistler wave beam, localized in the plane, transverse to the direction of propagation, becomes elliptically polarized and yields a significant longitudinal component E_z of electric field. Linear whistler wave beam propagation along the magnetic field (with frequency ω and parallel wave number k_z) is described by Maxwell equations

$$\nabla\times\mathbf{E}=-\frac{1}{c}\frac{\partial\mathbf{B}}{\partial t},\quad \nabla\times\mathbf{B}=\frac{1}{c}\frac{\partial\mathbf{D}}{\partial t}, \tag{A2}$$

where $\mathbf{D}(\omega,k_z)=\hat{\varepsilon}\mathbf{E}(\omega,k_z)$,

$$\hat{\varepsilon}=\begin{pmatrix}\varepsilon_\perp & ig & 0\\ -ig & \varepsilon_\perp & 0\\ 0 & 0 & \varepsilon_{||}\end{pmatrix},$$

and $\varepsilon_\perp=-\omega_{pe}^2/(\omega^2-\omega_{Be}^2)$, $\varepsilon_\parallel=-\omega_{pe}^2/\omega^2$, and $g=(\omega_{Be}/\omega)\omega_{pe}^2/(\omega^2-\omega_{Be}^2)$ are components of the dielectric tensor in the cold plasma approximation ($\omega\gg k_z v_{Te}$, where v_{Te} is the electron thermal velocity). We seek solutions of the system (A2) of the form $f(\mathbf{r}_\perp)\exp(-i\omega t+ik_z z)$. One can reduce the system (A2) to the set of equations for components $E_z(\mathbf{r}_\perp)$ and $B_z(\mathbf{r}_\perp)$ of the whistler wave field:

$$\left(\Delta_\perp+\frac{\omega^2}{c^2}\varepsilon_\perp-k_z^2\right)B_z+\frac{i\omega g}{ck_z}\left(\Delta_\perp+\frac{\omega^2}{c^2}\varepsilon_\parallel\right)E_z=0$$

$$\left[-k_z^2\varepsilon_\parallel+\varepsilon_\perp\left(\Delta_\perp+\frac{\omega^2}{c^2}\varepsilon_\parallel\right)\right]E_z+\frac{ik_z\omega}{c}gB_z=0.$$

Other components of the electromagnetic field can be found straightforwardly using Eqs. (A2). For a plane wave with $k_\perp=0$, this set yields two independent dispersion relations for the left- and right-hand polarized waves:

$$k_z^2-\frac{\omega^2}{c^2}\varepsilon_\perp=\pm\frac{\omega^2}{c^2}g.$$

However, they are coupled in the wave beam, where components B_z and E_z depend on transverse coordinates. Excluding B_z from the above set, we obtain one equation for the parallel component of the electric field:

$$\left[\left(-k_z^2-\frac{\varepsilon_\parallel}{\varepsilon_\perp}k_z^2+\frac{\omega^2}{c^2}(\varepsilon_\parallel+\varepsilon_\perp)-\frac{\omega^2}{c^2}\frac{g^2}{\varepsilon_\perp}\right)\Delta_\perp+\Delta_\perp^2 + \frac{\varepsilon_\parallel}{\varepsilon_\perp}\left\{\left(k_z^2-\frac{\omega^2}{c^2}\varepsilon_\perp\right)^2-\frac{\omega^4}{c^4}g^2\right\}\right]E_z=0. \tag{A3}$$

To restore the equation for a spatial-temporal evolution of the wave beam envelope, it is sufficient to put $k_z\to k_{z0}+i(\partial/\partial z)$, $\omega\to\omega_0-i(\partial/\partial t)$, supposing that the frequency ω_0 satisfies the dispersion relation (A1), and that corrections due to wave beam localization in the transverse direction are small (paraxial approximation). The term $\Delta_\perp^2 E_z$ formally corresponds to the fourth-order dispersion effect. The main nonlinear effect, connected with plasma electron heating, may be implemented in our model by replacing $\omega\to\omega_0+\omega_{nl}-i(\partial/\partial t)$, where (see Ref. [51])

$$\frac{\omega_{nl}}{\omega_0}=-\frac{\omega_0^2+\nu_e^2}{2\nu_e^2}\left(\sqrt{1+\frac{4\nu_e^2}{\omega_0^2+\nu_e^2}\left|\frac{E_z}{E_p}\right|^2}-1\right). \tag{A4}$$

For a steady-state wave propagation we put the operator $i(\partial/\partial t)$ equal to zero. Expanding expression (A4) up to terms of order $\sim|E_z/E_p|^4$ [where $E_p=\sqrt{3mT(\omega_0^2+\nu_e^2)\alpha}/e^2$, $\alpha\approx 2m/M$, ν_e is the effective frequency of electron collisions, T is the electron temperature], we obtain the corresponding nonlinear terms, which are to be added to Eq. (A3). Thus, wave beam propagation is described by GNSE (3), where $\Psi=E_z/F_0$, $F_0=\sqrt{12\pi T n_0\alpha}$, n_0 is the electron plasma density. For a stationary wave propagation, time t should be replaced by z in dimensionless GNSE (3). Here, dimensionless spatial coordinates z, x, y, are measured in units of c/ω_0. Coefficients of the GNSE are

$$D=\frac{\omega_0}{2\omega_{pe}}\left\{\left(\frac{\omega_{Be}}{2\omega_0}\right)^2-1\right\},\quad P=\frac{1}{8}\left(\frac{\omega_0}{\omega_{pe}}\right)^3,$$

$$B=-\left(\frac{\omega_{pe}}{\omega_0}\right)^3,\quad K=\frac{\nu_e^2}{\omega_0^2}\left(\frac{\omega_{pe}}{\omega_0}\right)^5. \tag{A5}$$

Note that dispersion of the perpendicular group velocity for whistlers ($\partial^2\omega/\partial^2 k_\perp^2$) changes its sign from plus to minus at $\omega_0\approx\omega_{Be}/2$ when frequency ω increases. However, to avoid a contradiction with our previous notations, we will still call the case $DB<0$ ($\omega<\omega_{Be}/2$) the normal dispersive regime and the case $DB>0$ ($\omega>\omega_{Be}/2$) the anomalous dispersive regime.

Let us compare our theoretical and experimental results of Ref. [3]. The stationary whistler wave self-focusing has been observed in both dispersive regimes (for $\omega<\omega_{Be}/2$ and for $\omega>\omega_{Be}/2$). Referring to the plasma parameters of the experimental setup [3], we obtain an estimate for the parameter $\kappa=KD^2/PB^2\approx(1-2)\times10^{-3}$. In normalized units, used for numerical calculations, the parallel whistler wavelength $\lambda_\parallel=10$ cm corresponds to the dimensionless parameter $\lambda_{\max}\approx 0.5$. Since the absolute value of the nonlinear shift of wave number should be much smaller than $\lambda_{\max}$, the experimental conditions correspond to the lower values of energy on

energy-dispersion diagrams $N(\lambda)$ [Figs. 2(b) and 8(b)], where they slowly change with λ. We find that the perpendicular scale of whistler waveguides is of the order of a few centimeters, which is in good agreement with the experimentally observed scale. However, the theoretical value of field amplitude is approximately ten times smaller than experimental values. This discrepancy may be connected with an underestimate of collision frequency (authors of Ref. [3] supposed it to be of the order of $\nu_e \approx 10^{-2}\omega_{Be}$, as for electron-neutral collision frequency). It gives a too small value for coefficient K of GNSE (3) and for normalization factor E_p, and therefore it gives understated values for the whistler intensity. Using larger values of the effective collision frequency, due to the anomalous scattering of electrons by wave fluctuations in turbulent plasma, one gets, accordingly, a larger estimate for a ducted whistler intensity.

[1] K. Longren and A. Scott, *Solitons in Action* (Academic Press, New York, 1978).
[2] H.C. Kim, R.L. Stenzel, and A.Y. Wong, Phys. Rev. Lett. **33**, 886 (1974).
[3] R.L. Stenzel, Phys. Fluids **19**, 865 (1976).
[4] S.V. Antipov, M.V. Nezlin, and A.S. Trubnikov, Physica D **1–2**, 311 (1981).
[5] D.L. Eggleston, A.Y. Wong, and C.B. Darrow, Phys. Fluids **25**, 257 (1982).
[6] T. Cho and S. Tanaka, Phys. Rev. Lett. **45**, 1403 (1980).
[7] H. Pecseli, B. Lybekk, J. Trulsen, and A. Eriksson, Plasma Phys. Controlled Fusion **39**, A227 (1997).
[8] A.A. Balmashnov, Phys. Lett. **79A**, 402 (1980).
[9] J.E. Maggs, G.J. Morales, and W. Gekelman, Phys. Plasmas **4**, 1881 (1997).
[10] L.F. Mollenauer, R.H. Stolen, and J.P. Gordon, Phys. Rev. Lett. **45**, 1095 (1980).
[11] G.P. Agrawal, *Nonlinear Fiber Optics* (Academic Press, New York, 1995).
[12] A. Hasegawa, Phys. Plasmas **8**, 1763 (2001).
[13] G.A. Swartzlander, Jr. and C.T. Law, Phys. Rev. Lett. **69**, 2503 (1992).
[14] B. Luther-Davies and Y.S. Kivshar, Phys. Rep. **298**, 81 (1998).
[15] V. Tikhonenko, J. Christou, and B. Luther-Davies, Phys. Rev. Lett. **76**, 2698 (1996).
[16] Y.S. Kivshar and D.E. Pelinovsky, Phys. Rep. **331**, 117 (2000).
[17] B.A. Kalinikos, N.G. Kovshikov, and A.N. Slavin, JETP Lett. **38**, 413 (1983).
[18] A.S. Davydov, *Solitons in Molecular Systems* (Kluwer Academic Press, Dordrecht, 1985).
[19] L. Cruzeiro *et al.*, Phys. Rev. A **37**, 880 (1988).
[20] Yu.B. Gaididei *et al.*, Phys. Scr., T **T67**, 151 (1996).
[21] L. Brizhik, A. Eremko, B. Piette, and W.J. Zakrzewski, Physica D **159**, 71 (2001).
[22] P.G. Kevrekidis, Yu.B. Gaididei, A.R. Bishop, and A. Saxena, Phys. Rev. E **64**, 066606 (2001).
[23] L. Bergé and J.J. Rasmussen, Phys. Plasmas **3**, 824 (1996).
[24] N. Vakhitov and A. Kolokolov, Izv. Vyssh. Uchebn. Zaved., Radiofiz. **17**, 1332 (1974).
[25] F. Vidal and T.W. Johnston, Phys. Rev. Lett. **77**, 1282 (1996).
[26] K.H. Spatschek, Fortschr. Phys. **35**, 491 (1987).
[27] K. Dimitrevski *et al.*, Phys. Lett. A **248**, 369 (1998).
[28] T.A. Davydova and A.I. Fishchuk, Phys. Lett. A **245**, 453 (1998).
[29] T.A. Davydova and A.I. Fishchuk, Ukr. Fiz. Zh. **40**, 487 (1995).
[30] T.A. Davydova and Yu.A. Zaliznyak, Phys. Scr. **61**, 476 (2000).
[31] W. Krolikovski, O. Bang, J.J. Rasmussen, and J. Wyller, Phys. Rev. E **64**, 016612 (2001).
[32] V.I. Karpman, Phys. Lett. A **160**, 531 (1991).
[33] V.I. Karpman, Phys. Rev. E **53**, 1336 (1996).
[34] Yu.A. Zaliznyak, T.A. Davydova, and A.I. Yakimenko, Nonlinear Processes in Geophysics **9**, 125 (2002).
[35] D. Mihalache, D. Mazilu, I. Towers, B.A. Malomed, and F. Lederer, J. Opt. A, Pure Appl. Opt. **4**, 615 (2002).
[36] T.A. Davydova and Yu.A. Zaliznyak, Physica D **156**, 260 (2001).
[37] V.E. Zakharov and E.A. Kuznetsov, JETP **86**, 1035 (1998).
[38] J.J. Rasmussen and K. Rypdal, Phys. Scr. **33**, 481 (1986).
[39] S.K. Turitsyn, Theor. Math. Phys. **64**, 226 (1985).
[40] A. Höök and M. Karlsson, Opt. Lett. **18**, 1388 (1993).
[41] D. Anderson, Phys. Rev. A **27**, 3135 (1983).
[42] H. Michinel *et al.*, Phys. Rev. E **65**, 066604 (2002).
[43] E.A. Kuznetsov, A.M. Rubenchik, and V.E. Zakharov, Phys. Rep. **142**, 103 (1986).
[44] V.I. Petviashvili and V.V. Yan'kov, in *Solitons and Turbulence*, edited by B.B. Kadomtsev, Reviews of Plasma Physics (Consultants Bureau, New York, 1989), pp. 1–62.
[45] D.V. Skryabin and W.J. Firth, Phys. Rev. E **58**, 3916 (1998).
[46] B.A. Malomed, L.-C. Crasovan, and D. Mihalache, Physica D **161**, 187 (2002).
[47] V.L. Berezhiani, V. Skarka, and N.B. Aleksic, Phys. Rev. E **64**, 057601 (2001).
[48] I. Towers *et al.*, Phys. Lett. A **288**, 292 (2001).
[49] D. Mihalache *et al.*, Phys. Rev. Lett. **88**, 073902 (2002).
[50] D. Mihalache *et al.*, Phys. Rev. E **66**, 016613 (2002).
[51] A.V. Gurevich and A.B. Shvarzburg, *Nonlinear Theory of Radiowave Propagation in Ionosphere* (Nauka, Moscow, 1973) (in Russian).